16th World Congress in Computational Mechanics (WCCM)
21-26 July 2024, Vancouver, Canada
A. Korobenko, M. Laforest, S. Prudhomme, R. Vaziri (Eds)

FATIGUE CRACK PROPAGATION BEHAVIOR ANALYSIS OF 15MnTi STEEL BASED ON CYCLIC COHESION MODEL

JINGYI GUO[1], JIAN HE [2] AND XIAODAN SUN[3]

[1]College of Aerospace and Civil Engineering
145 Nantong Street, Harbin, Harbin Engineering University 150001, China
gjy021808@hrbeu.edu.cn

[2] College of Aerospace and Civil Engineering
145 Nantong Street, Harbin, Harbin Engineering University 150001, China
hejian@hrbeu.edu.cn

[3] College of Aerospace and Civil Engineering
145 Nantong Street, Harbin, Harbin Engineering University 150001, China
sunxiaodan@hrbeu.edu.cn

Key words: 15MnTi, CCZM, Fatigue Crack, Crack Propagation.

Abstract. *15MnTi steel is widely used in high load structures such as bridges, pressure vessels, ships, and vehicles due to its excellent mechanical properties. In the course of service, the failure of steel structure is mostly caused by fatigue fracture. In order to investigate the crack growth of 15MnTi steel under fatigue load, the cohesive zone model (CZM) was used to simulate the crack growth. The CZM can simulate brittle and plastic fracture behavior by using the function of crack interface opening force and opening displacement to avoid the stress singularity of crack tip. On this basis, a cyclic cohesive zone model (CCZM) was established to study the fatigue crack propagation behavior. This model effectively links damage, tractive force, and cumulative displacement while incorporating the process of fatigue crack growth to accurately simulate material damage evolution under fatigue load. Experimental studies on crack growth in 15MnTi steel at three stress ratios reveal a linear relationship between crack growth rate and stress intensity factor range for different stress ratios. The parameters of Paris formula were calculated using crack growth rate and stress intensity factor range, which provided reference for the selection of model parameters. By utilizing the user element subroutine (UEL) in Abaqus and compiling the CCZM using Fortran language specifically for 15MnTi steel, simulations were conducted to analyze the evolution of crack tip state under various stress ratios and discuss the corresponding crack growth behavior based on experimental observations. The results demonstrate that the fatigue crack propagation rate varies linearly with both stress ratio range and stress intensity factor range, consistent with experimental findings. The results of the opening and closing evolution of the crack tip are consistent with the law of crack propagation, which indicates that the plastic behavior of the*

crack tip can be effectively characterized by the CCZM. Furthermore, parameters obtained from the cyclic cohesive zone model's Paris formula closely match experimental data, thus validating its accuracy and feasibility in simulating fatigue crack propagation behavior.

1 INTRODUCTION

With the rapid development of computers, numerical simulation methods were widely used in the study of crack propagation. After continuous research by scholars, the commonly used methods for the initiation and dynamic propagation of cracks include the preset crack path method [1], the grid re-division method [2], the extended finite element method [3], and the cohesive zone model (CZM) method. Compared with other methods, the advantage of the CZM is that it utilizes the function of crack interface opening force and opening displacement to avoid stress singularity at the crack tip, simulate brittle fracture behavior and plastic fracture behavior.

In 1963, Paris [4] proposed the Paris formula based on fracture mechanics theory, which can describe the law of crack propagation. Most research on the law of fatigue crack propagation is also based on this formula. Radon et al. [5] observed a typical linear relationship between crack propagation length and number of cycles through cyclic tensile experiments, based on the concept of linear elastic fracture mechanics. Liu et al. [6] extended the Paris formula, explaining the essence of crack propagation from a microscopic perspective and endowing the material parameters in the Paris formula with clear physical meanings, providing a theoretical basis for subsequent research on this formula. Park et al. [7] treated C as a random variable and m as a constant, based on the Paris formula. The probability distribution of fatigue crack propagation resistance has been determined.

Nguyen [8] established a cohesive force model based on the cohesive theory of fracture and successfully simulated fatigue crack propagation. Goyal et al. [9] considered the impact of unloading process on fatigue process and extended the existing cohesive zone model to achieve damage calculation during unloading process. Pereira [10] used a cyclic cohesive zone model to consider the accumulation of loading and unloading damage at the crack front, achieving crack propagation life prediction. Yang [11] developed a user element subroutine (UEL) for scaled boundary finite element methods for general static and dynamic stress analysis and validated it through examples.

In summary, although many scholars have conducted numerical simulations on crack propagation behavior, there are few detailed analyses and studies on crack propagation laws based on cyclic cohesion models that consider fatigue damage evolution. And develop a UEL subroutine to simulate fatigue crack propagation behavior based on the cyclic cohesion model proposed by Roe [12], Xu and Needleman [13]. By comparing with experimental results, the feasibility and accuracy of studying fatigue crack propagation behavior based on cohesive force model are verified.

2 FATIGUE CRACK PROPAGATION EXPERIMENT OF 15MNTI STEEL

Table 1 shows the basic mechanical property parameters of 15MnTi steel, which has good strength and plasticity, so it is often used for supporting structures of equipment in chemical industry, ships and pressure vessels.

Table 1: Material Parameters

Young's Modulus E(GPa)	Yield Strength σ_s (MPa)	Poisson's ratio v	density ρ (kg/m^3)	Specific Heat Capacity C[J/(kg·K)]
210	638	0.3	7850	500

To analyze the effect of stress ratio on the fatigue crack propagation rate of 15MnTi steel, compact tensile experiments were conducted with stress ratios of R = 0.1, 0.2, and 0.5. Based on experimental measurements of crack length and corresponding loads, the crack propagation rate *(da/dN)* was calculated using the secant method. Fig.1 shows the linear fitting results of lg*(da/dN)*-lg*(ΔK)* under different stress ratios.

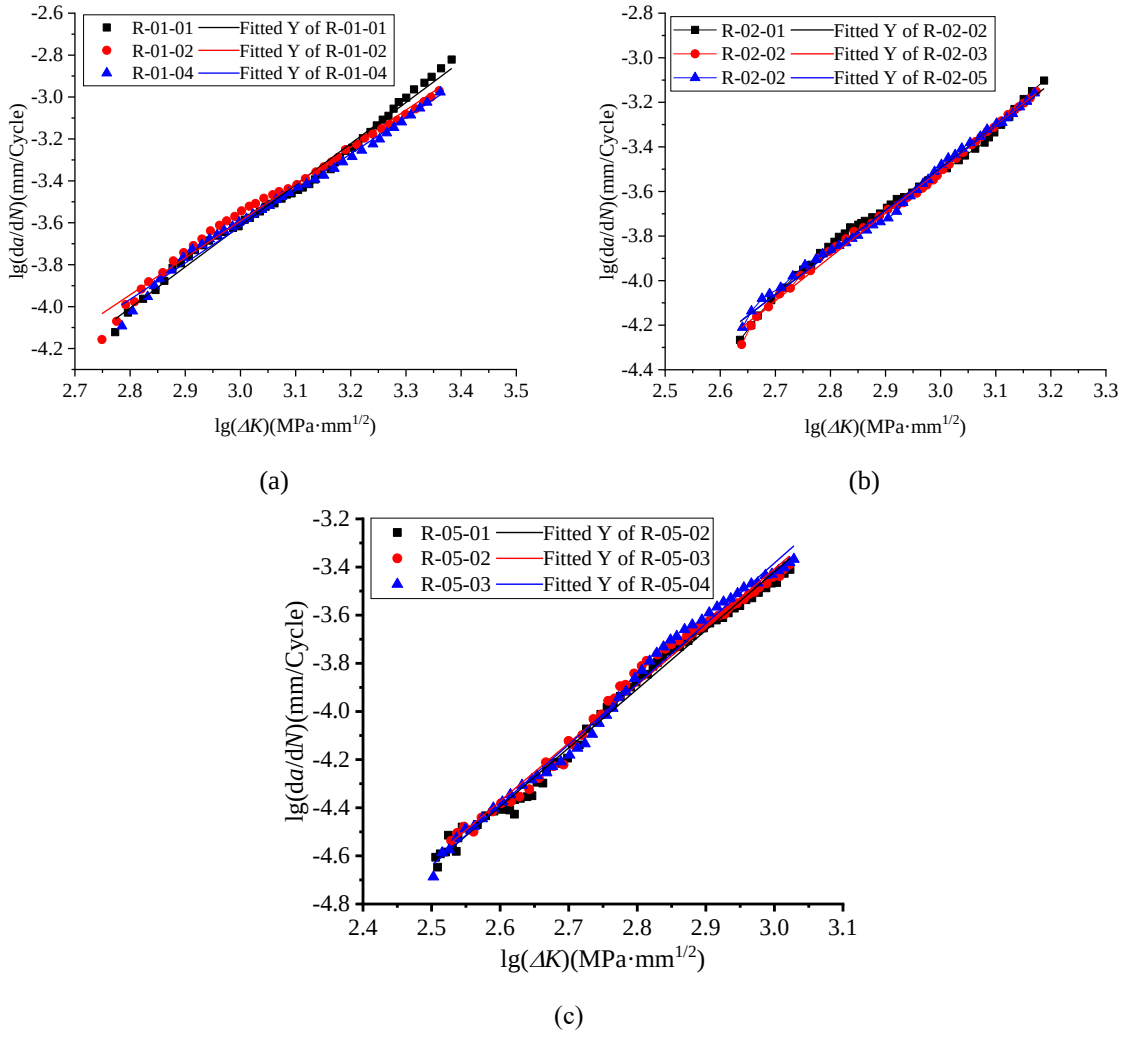

Figure 1: Relationship between crack propagation rate and stress intensity factor range under different stress ratios: (a) R = 0.1, (b) R = 0.2, (c) R = 0.5

In Fig. 1, there is a significant linear relationship between crack propagation rate and stress intensity factor range under different stress ratios, and the fatigue crack propagation rate increases with the increase of stress intensity factor range. According to the basic form of the Paris formula, taking the logarithm on both sides of the equation yields:

$$\lg\left(da/dN\right)=\lg C+m\lg\Delta K \tag{1}$$

The paper selects the single specimen method and obtain the parameter C of the Paris formula through linear regression m. As shown in Table 2:

Table 2: Average values of Paris formula parameters under different stress ratios

Stress ratio R	Average value of parameter C	Average value of parameter m	Paris formula
0.1	1.4108×10^{-9}	1.7495	$(da/dN)_{ave}=1.4108\times10^{-9}\Delta K^{1.7495}$
0.2	5.6938×10^{-10}	1.9158	$(da/dN)_{ave}=5.6938\times10^{-10}\Delta K^{1.9158}$
0.5	1.7033×10^{-11}	2.4551	$(da/dN)_{ave}=1.7033\times10^{-11}\Delta K^{2.4511}$

3 NUMERICAL SIMULATION OF FATIGUE CRACK PROPAGATION BEHAVIOR

3.1 Fatigue cumulative damage criterion

Unlike conventional crack propagation problems, loading or unloading and damage evolution are key considerations [14] for fatigue crack propagation problems. To accurately describe the damage evolution behavior of elements under fatigue loading, these two rules are introduced into the cyclic cohesion zone model.

Under tensile load, there is a relationship between the traction force T_n and the opening displacement Δ_n as follows:

$$T_n=\sigma_{\max,0}\left(\frac{\Delta_n}{\delta_0}\right)\exp\left(1-\frac{\Delta_n}{\delta_0}\right) \tag{2}$$

where, $\sigma_{\max,0}$ represents the initial strength without damage, δ_0 is the feature length corresponding to $\sigma_{\max,0}$. After considering the evolution of damage, the real-time strength of cohesive units will continuously decrease due to damage. The real-time strength $\sigma_{\max}$ during the damage evolution process needs to be continuously updated based on the degree of damage to the unit at this time. The calculation of real-time strength of cohesive units is in Eq. (3):

$$\sigma_{\max}=\sigma_{\max,0}(1-D_c) \tag{3}$$

For the calculation of the damage variable $\dot{D}_c$ is shown in Eq. (4):

$$\begin{cases} \dot{D}_c = \dfrac{\partial D}{\partial t} = \dfrac{|\dot{\Delta}_n|}{\delta_\Sigma}\left(\dfrac{T_n}{\sigma_{\max}} - C_f\right)H(\Delta - \delta_0) \\ \dot{D}_c \geq 0, \Delta = \int_t \left|\dot{\Delta}_n\right| dt \end{cases} \tag{4}$$

where, $\dot{D}_c$ represents the cumulative rate of fatigue damage; Δ_n is the normal opening displacement; Δ is the cumulative opening displacement; σ_f is the durability limit of cohesive units; C_f represents the durability coefficient, $(C_f = C_f / \sigma_{\max,0})$. δ_Σ is the cumulative cohesive unit length, usually set as an integer multiple of the characteristic length δ_0, and used to normalize the effective opening displacement increment of the material. The function H is a step function, which represents that when Δ is greater than δ_0, the cumulative fatigue calculation rate is only greater than 0, indicating that the element begins to experience fatigue damage.

The cyclic loading process can cause changes in the stiffness of the elements, thereby altering the loading or unloading path. The relationship between traction force and opening displacement can be explained by Eq. (5) for this mechanical behavior:

$$T_n = T_{n,\max} + K_n(\Delta_n - \Delta_{n,\max}) \tag{5}$$

where, $T_{n,\max}$ is the maximum normal tension of the cohesive model; $\Delta_{n,\max}$ is the maximum normal opening amount of the cohesive model; K_n is the normal stiffness of the cohesive model $(K_n = T_{n,\max} / \Delta_{n,\max})$;

During the process of continuous opening and closing of cracks, maybe $\Delta_n \leq 0$, which means $T_n < 0$, indicating a state of crack compression. At this point, if the cumulative damage variable of the interface element reaches the critical value of 1, it indicates that the interface element has completely failed and there is contact on both sides of the crack surface. When the interface unit is in such a state, the relationship between traction and opening displacement will follow the relationship shown in Eq. (6).

$$T_n = \alpha\sigma_{\max,0}\left(\frac{\Delta_n}{\delta_0}\right)\exp\left(1 - \frac{\Delta_n}{\delta_0}\right) \tag{6}$$

It should be noted that when the crack interface is in a compressed state, the initial strength of the undamaged element needs to be multiplied by the penalty stiffness coefficient of the larger cohesive element. In this paper, $\alpha = 30$ [15].

3.2 Algorithm Implementation of CCZM

For the cyclic cohesive zone model developed in this study, the fatigue cumulative damage criterion and cyclic loading criterion are written into finite element software using Fortran language. The normal opening displacement of Gaussian points is calculated based on coordinate transformation matrix and element node displacement. The unit damage variable D is calculated through intermediate state variables to determine the state of the unit. Fig. 2 is

the algorithm flowchart of the cyclic cohesion zone model.

To improve computational efficiency and consider the symmetry of the model, the process of model establishment and mesh division were optimized. The final crack propagation path and local refinement mesh are shown in Fig. 3.

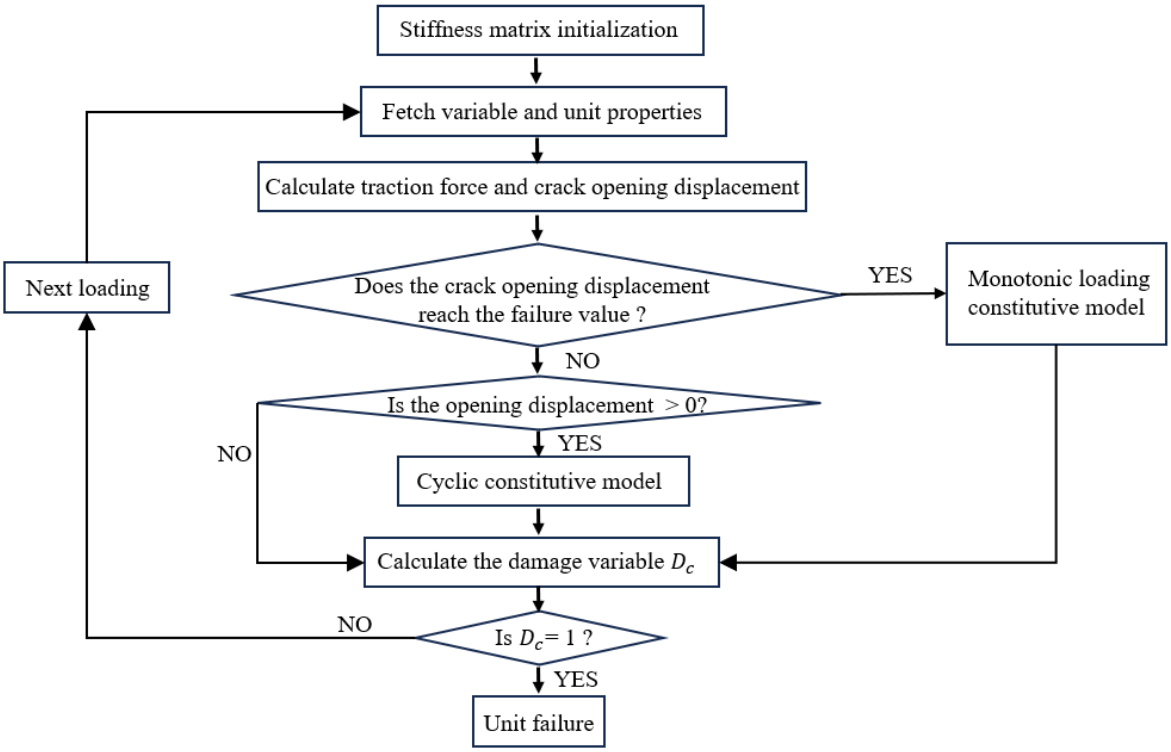

Figure 2: Algorithm flow of the cyclic cohesion model

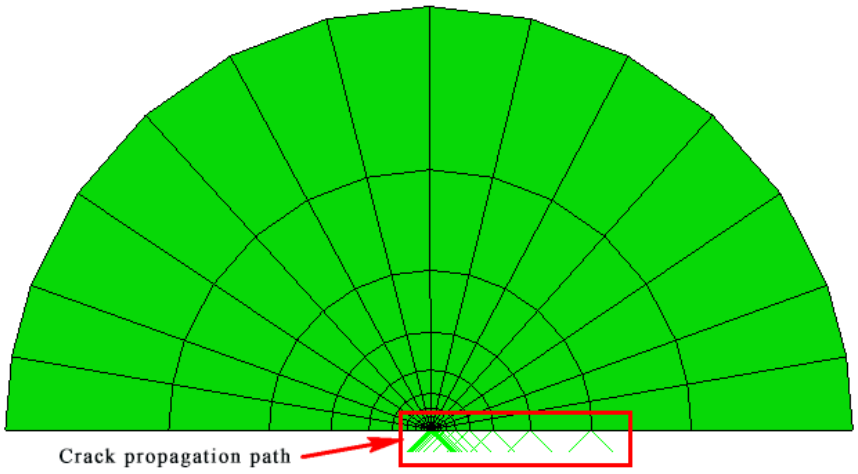

(a) Crack propagation path

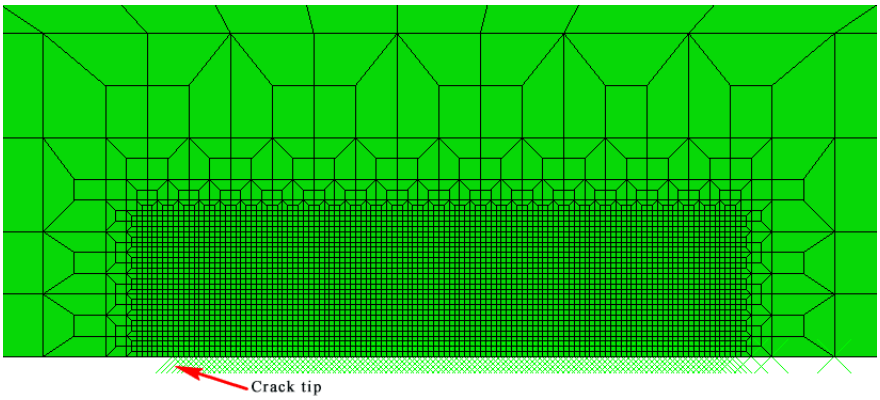

(b) Local refinement mesh

Figure 3: Finite element model

For a set of horizontal element nodes adjacent to a 4-node line element with 0 thickness, the degrees of freedom in the *X* and *Y* directions are restricted.The periodic displacement boundary conditions that vary with time are applied to the outer boundary of the model [15]:

$$\begin{pmatrix} u_x(t) \\ u_y(t) \end{pmatrix} = \frac{K_I}{2\mu}\sqrt{\frac{2r}{\pi}} \times \begin{pmatrix} \cos\frac{\theta}{2}\left[\frac{(3-4\upsilon-1)}{2}+\sin^2\frac{\theta}{2}\right] \\ \sin\frac{\theta}{2}\left[\frac{(3-4\upsilon-1)}{2}-\cos^2\frac{\theta}{2}\right] \end{pmatrix} \tag{7}$$

where, (r,θ) is the coordinates of the outer boundary nodes of the finite element model in polar coordinates, K_I is the stress intensity factor.

The acquisition of cohesion model parameters usually requires continuous adjustment based on experimental and numerical simulation results [16]. In the study, the parameters of the cyclic cohesion model used to simulate fatigue crack propagation behavior were calibrated based on the experimental results of fatigue crack propagation, as shown in Table 3.

Table 3: Parameters of the CCZM used for simulating fatigue crack propagation behavior

$\sigma_{max,0}$ (MPa)	δ_0 (μm)	δ_Σ (μm)	Φ_n (KJ/m^2)	C_f
2600	3.5	17.5	24.74	0.28

4 ANALYSIS OF FATIGUE CRACK PROPAGATION LAW

In order to investigate the changes in the open and closed state of the free surfaces on both sides of the crack tip during crack propagation, the crack tip opening displacement of each cohesive unit along the crack propagation path was extracted when the crack tip extended to different positions. Fig. 4 shows the numerical simulation results of the crack closure and opening states at different cycles when the crack propagates to 1.6 mm within a fixed stress intensity factor range under three different stress ratios.

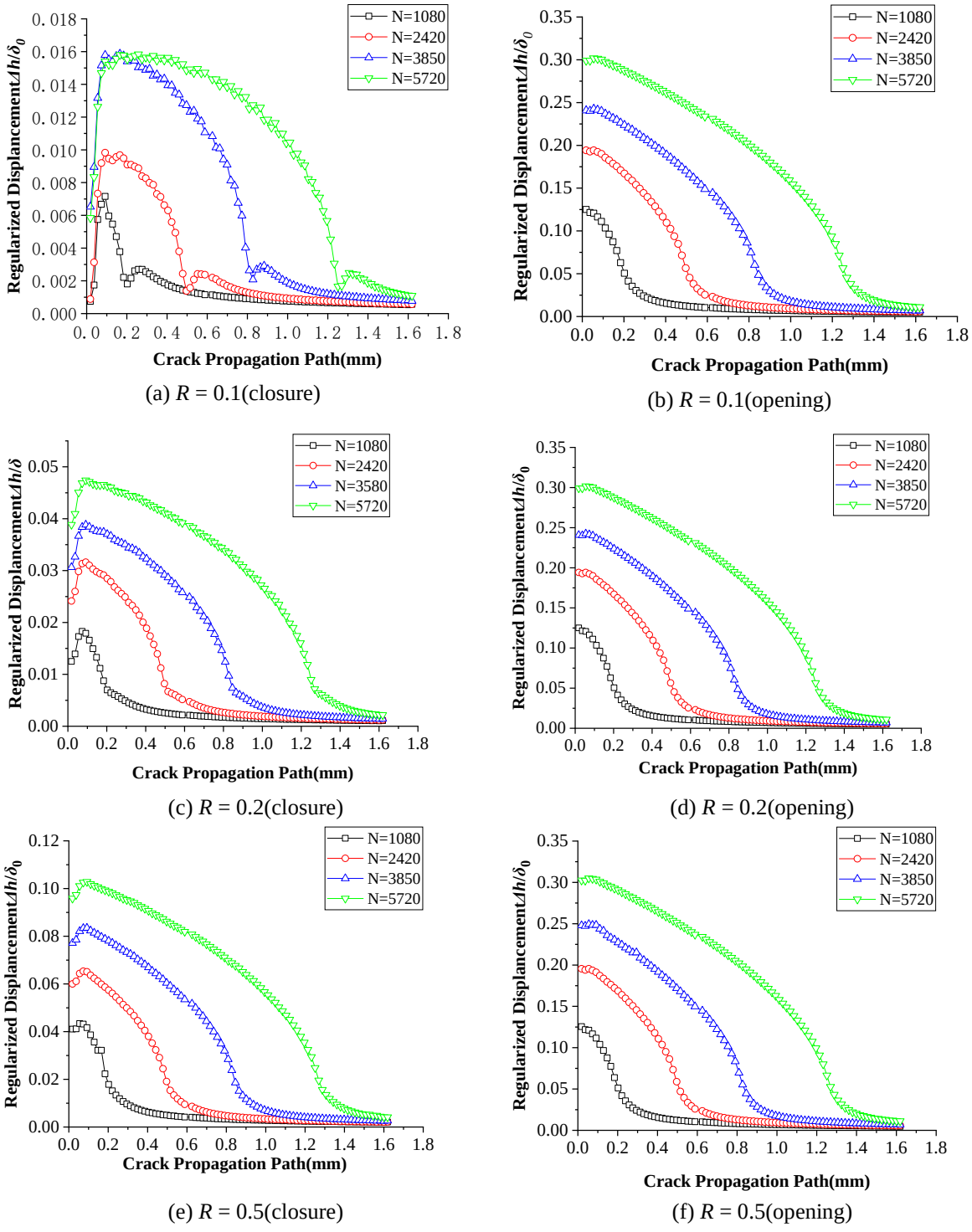

(a) R = 0.1(closure)

(b) R = 0.1(opening)

(c) R = 0.2(closure)

(d) R = 0.2(opening)

(e) R = 0.5(closure)

(f) R = 0.5(opening)

Figure 4: Crack tip state under different stress ratios

Compared with the crack tip opening and closing states at R = 0.1, 0.2, and 0.5, the maximum regularized opening displacement during the crack opening process is almost not affected by

the stress ratio. However, during the crack closure process, the maximum regularized opening displacement increases as the stress ratio gradually increases. This is because when the range of stress intensity factors remains constant, the maximum cyclic load at R = 0.5 is maximum, and the plastic deformation at the crack tip caused by stress concentration increases with the increase of maximum load [17].

Unlike elastic deformation, plastic deformation is an irreversible process, so even if the crack is in a closed state, the opening displacement caused by plastic deformation will increase with the increase of maximum load. At the same time, the increase in stress ratio leads to an increase in the minimum stress of fatigue load. The increased stress cancels out the residual compressive stress at the crack tip, weakening the crack closure effect [18]. Therefore, based on the opening and closing evolution law of the crack tip, it can be verified that the cyclic cohesive force model can simulate the plastic behavior of fatigue crack propagation.

To investigate the influencing factors of crack propagation rate, several groups of numerical simulations were conducted on the fatigue crack propagation process under different stress intensity factor amplitudes and stress ratios. Fig. 5 shows the relationship between the stress intensity factor range and crack propagation rate at stress ratios R of 0.1, 0.2, and 0.5, respectively.

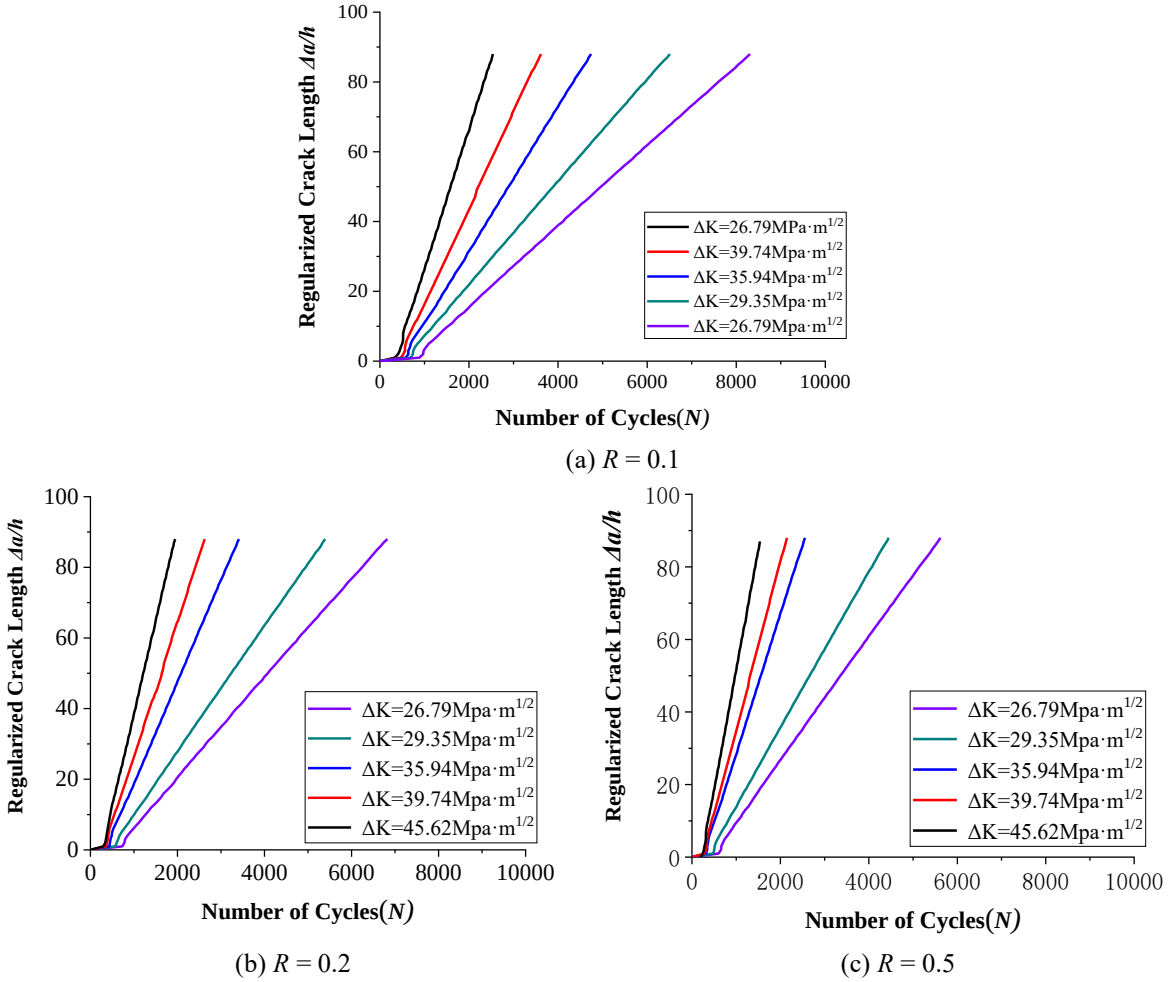

(a) R = 0.1

(b) R = 0.2

(c) R = 0.5

Figure 5: Crack propagation rate under different stress ratios

In Fig. 5, it can be observed that the range of stress intensity factors and stress ratios both affect the crack propagation rate, and the fatigue crack propagation rate increases more significantly in the high stress intensity factor range than in the low stress intensity factor range.

The relationship between the stress intensity factor range and crack propagation rate at stress ratios R of 0.1, 0.2, and 0.5 obtained through experiments and numerical simulations is shown in Fig. 6.

Fit the results of simulating crack propagation behavior using the cyclic cohesive force unit and determine the parameters of the Paris formula, as shown in Table 4.

Overall, the trend of the parameters obtained from numerical simulation fitting with stress ratios of R = 0.1, 0.2, and 0.5 is consistent with the trend of the material parameters obtained from experiments with stress ratios

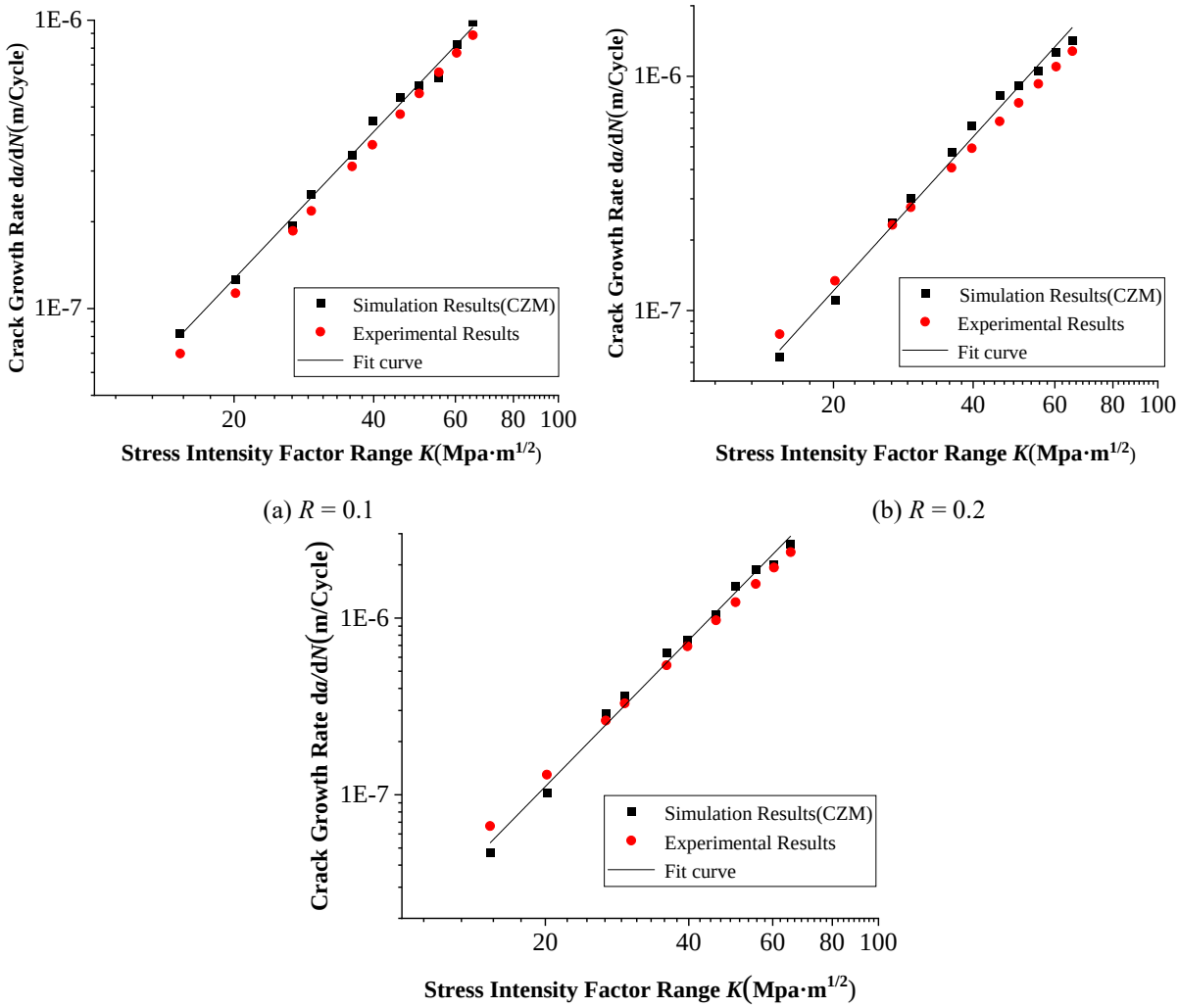

(a) R = 0.1 (b) R = 0.2

(c) R = 0.5

Figure 6: *da/dN* - *ΔK* Relationship under Different Stress Ratios

Table 4 Paris Formula Parameters

Stress ratio R	Experimental value of parameter C	Experimental value of parameter m	Simulated value of parameter C_{FEM}	Simulated value of parameter M_{FEM}	Correlation coefficient r
0.1	1.4108×10^{-9}	1.7495	7.616×10^{-10}	1.7068	0.9960
0.2	5.6938×10^{-10}	1.9158	1.760×10^{-10}	2.1824	0.9910
0.5	1.7033×10^{-11}	2.4551	2.925×10^{-11}	2.7520	0.9918

5 CONCLUSIONS

- The results of both experiments and numerical simulations indicate that as the stress ratio R increases from 0.1 to 0.5, the fatigue crack propagation rate parameter C decreases, while the fatigue crack propagation parameter m increases.
- The results of applying the cyclic cohesion model to the evolution of crack tips conform to the law. The fatigue crack propagation rate of 15MnTi steel shows a linear relationship with the change of stress ratio and stress intensity factor range, increasing with the increase of both. Moreover, the fatigue crack propagation rate increases more significantly in the high stress intensity factor range than in the low stress intensity factor range.
- The Paris material parameter C obtained through the cyclic cohesion model remains on the same order of magnitude as the experimental results except for R = 0.1. The errors between parameter m and experimental results are 2.5%, 12%, and 10.8%, respectively, all of which do not exceed 15%. The above results verify the correctness of subroutine compilation, the rationality of parameter selection for the cyclic cohesion model, and the accuracy of simulating fatigue crack propagation behavior based on the cyclic cohesion model.

ACKNOWLEDGEMENT

This paper is funded by the International Exchange Program of Harbin Engineering University for Innovation-oriented Talents Cultivation.

REFERENCES

[1] M. G. A. Tijssens, B. L. J. Sluys, E. Van der Giessen, Numerical simulation of quasi-brittle fracture using damaging cohesive surfaces. *European Journal of Mechanics, A/Solids* **19**, 761-779 (2000).

[2] H. Proudhon *et al.*, 3D simulation of short fatigue crack propagation by finite element crystal plasticity and remeshing. *International Journal of Fatigue* **82**, 238-246 (2016).

[3] Afshar, A. Daneshyar, S. Mohammadi, XFEM analysis of fiber bridging in mixed-mode crack propagation in composites. *Composite Structures* **125**, 314-327 (2015).

[4] P Paris, F Erdogan. A critical analysis of crack propagation laws. *ASME Transactions, Journal of Basic Engineering, Series* D, **85 D (4)**: 528~534(1963).

[5] Radon J C, Culver L E. Fatigue-crack propagation in metals. *Experimental Mechanics*, **16(3)**: 105-110(1976),.

[6] L. Liming, D. Menglan, L. Chuntu, Z. Huijuan, ON THE PHYSICAL NATURE OF THE PARIS LAW.

Chinese Journal of Theoretical and Applied Mechanics, 171-175 (2003).

[7] U. H. Park, H. W. Lee, S. J. Kim, C. R. Lee, J. H. Kim, Stochastic characteristics of fatigue crack growth resistance of SM45C steel. *International Journal of Automotive Technology* **8**, 623-628 (2007).

[8] O. Nguyen, E. A. Repetto, M. Ortiz, R. A. Radovitzky, A cohesive model of fatigue crack growth. *International Journal of Fracture* **110**, 351-369 (2001).

[9] V. K. Goyal, E. R. Johnson, in *44th AIAA/ASME/ASCE/AHS/ASC Structures, Structural Dynamics, and Materials Conference, April 7, 2003 - April 10, 2003*. (American Inst. Aeronautics and Astronautics Inc., Norfolk, VA, United states, 2003), vol. 4, pp. 2514-2524

[10] K. Pereira, M. Abdel Wahab, Fretting fatigue lifetime estimation using a cyclic cohesive zone model. *Tribology International* **141**, (2020).

[11] Z. J. Yang, F. Yao, Y. J. Huang, Development of ABAQUS UEL/VUEL subroutines for scaled boundary finite element method for general static and dynamic stress analyses. *Engineering Analysis with Boundary Elements* **114**, 58-73 (2020).

[12] K. L. Roe, T. Siegmund, An irreversible cohesive zone model for interface fatigue crack growth simulation. *Engineering Fracture Mechanics* **70**, 209-232 (2003).

[13] X. P. Xu, A. Needleman, Void nucleation by inclusion debonding in a crystal matrix. *Modelling and Simulation in Materials Science and Engineering* **1**, 111-111 (1993).

[14] M. Yatomi, K. M. Nikbin, N. P. O'Dowd, Creep crack growth prediction using a damage based approach. *International Journal of Pressure Vessels and Piping* **80**, 573-583 (2003).

[15] Wang, T. Siegmund, A numerical analysis of constraint effects in fatigue crack growth by use of an irreversible cohesive zone model. *International Journal of Fracture* **132**, 175-196 (2005)

[16] X. Chen, *Numerical Study of Stable Tearing Crack Growth Events Using the Cohesive Zone Model Approach*. (2013)

[17] V. Iasnii, P. Yasniy, Influence of stress ratio on functional fatigue of pseudoelastic NiTi alloy. *Procedia Structural Integrity* **16**, 67-72 (2019)

[18] X. P. Zhang, C. H. Wang, L. Ye, Y. W. Mai, A study of the crack wake closure/opening behaviour of short fatigue cracks and its influence on crack growth. *Materials Science and Engineering: A* **406**, 195-204 (2005)